2015 International Symposium on Nonlinear Theory and its Applications
NOLTA2015, Kowloon, Hong Kong, China, December 1-4, 2015

Computational simulation: Local inhibitory synapses activate cortical regions around the lesion

Hiroyuki Kitano†, Katsuhiko Hata†, Yuta Kakimoto†, Tomokazu Urakawa† and Osamu Araki†

†Department of Applied Physics, Tokyo University of Science
6-3-1 Niijuku, Katsushika, Tokyo 125-8585, Japan
Email: j1515610@ed.tus.ac.jp, kansuke0731@mail.goo.ne.jp, ykaki@rs.kagu.tus.ac.jp, turakawa@rs.tus.ac.jp, brainics@rs.kagu.tus.ac.jp

Abstract– It has been known that the neural activity around the cortical lesion tends to arise. We simulated this phenomenon using a neural network model composed of excitatory and inhibitory neurons with strong-sparse and weak-dense connections, whose inhibitory ones are projected on neighboring neurons. Increased average membrane potentials in perilesional neurons were observed after damaging the injury. It is suggested that the activated neurons have lost more inhibitory projections from the neighboring injured region than excitatory ones.

1. Introduction

After a part of the central nervous system is injured in animal physiology experiments, some motor functions have been reported to recover spontaneously after a certain period of time [1,2]. This will be due to the remodeling function of neuronal circuitry with sprouting new axons.

When the rat loses the limb motor function because of the damage of the motor cortex, it has been reported that the neuronal activity around the lesion in the cortex is increased [3]. And it is also reported that the dominant area of the limb motor function is moved from the injured region to the peripheral or contralateral region after that and the lost function is restored after all. However, the recovery function was blocked when the perilesional activities were artificially suppressed. This suggests that the regional activation around the injury plays an important role in the recovery process. On the other hand, modeling studies have been attempted to elucidate the mechanism of remodeling of cortices after injury in recent years [4,5]. However, the mechanism of increased activity around the injury has not been elucidated yet, since the cost of physiological experiments is generally huge. Thus the purpose of this study is to show that a strong-sparse and weak-dense (SSWD) neural network model with local inhibitory synaptic connections enables neural activities around the lesion to increase. This idea is one proposal for neural recovery mechanism.

2. Methods

2.1. Strong-sparse and weak-dense network model

Based on the SSWD model proposed by Teramae et al. [6], we have made the projection range of the inhibitory neurons more local. The neurons of SSWD fire spontaneously even without external inputs and their average firing rates are mostly uniform. SSWD model produces spontaneous firings similar to those observed in real brains in that the variance of EPSP (excitatory postsynaptic potential) in cortical cells is quite large. For this purpose, the synaptic weights from excitatory to excitatory neurons are determined so that the distribution of maximum values of the EPSPs approximately follows the lognormal distribution. In our simulations, we injure a part of the spontaneously firing neurons and clarify the changes of firings after the injury.

First, we will show the model neuron. The membrane potential of a model neuron follows the following equation [6]:

$$\frac{dv}{dt} = -\frac{1}{\tau_m}(v - V_L) - g_E(v - V_E) - g_I(v - V_I), \qquad (1)$$

where v is the membrane potential, g_E and g_I are excitatory and inhibitory synaptic conductance respectively, and the membrane time constant τ_m is 20 ms for excitatory neurons and 10 ms for inhibitory neurons. The reversal potentials for leak, excitatory and inhibitory postsynaptic currents are $V_L = -70$ mV, $V_E = 0$ mV, $V_I = -80$ mV, respectively. The spike threshold is $V_{thr} = -50$ mV, and the reset value after firing is $V = -60$ mV. Further, refractory period is 1 ms. External inputs composed of Poisson spike trains fire the neurons for 100 ms in the beginning of the simulation. As one of the important features, this model retains spontaneous firings without bursts even after the external inputs are stopped.

In response to input spikes, excitatory synaptic conductance g_E and inhibitory synaptic conductance g_I for a neuron change in accordance with the following equation [6]:

$$\frac{dg_X}{dt} = -\frac{g_X}{\tau_s} + \sum_j G_{X,j} \sum_{s_j} \delta(t - s_j - d_j)\,(X = E, I), \qquad (2)$$

where G_j is the conductance weight of received spikes from the j-th neuron, $\delta(t)$ is the delta function, d_j is the transmission delay from the j-th neuron, and s_j is a spike timing of the j-th presynaptic neuron. The decay constant τ_s is 2 ms, and synaptic delays are chosen randomly between $d_0 - 1$ to $d_0 + 1$ ms: $d_0 = 2$ for excitatory-to-

excitatory connections and $d_0 = 1$ for the other connection types.

Since EPSP is the postsynaptic membrane potential v after an input spike, it is calculated by the Eqs.(1) and (2). Thus, the conductance weight $G_{E,j}$ essentially affects the value of EPSP. To make the maximum values of EPSPs follow the lognormal distribution (Eq.(3)), the values of $G_{E,j}$ between excitable cells were stochastically decided.

$$p(x) = \frac{\exp\left[-\frac{(\log x - \mu)^2}{2\sigma^2}\right]}{\sqrt{2\pi}\sigma x} \qquad (3)$$

where $\mu = \log 0.2 + 1, \sigma = 1$

When some $G_{E,j}$ values are larger for a neuron, responsive EPSPs tend to be larger even if there is a small number of input connections. Conversely, when $G_{E,j}$ values are smaller, the impact of spikes is quite small even with a large number of connections. All conductance weights except excitatory-to-excitatory connections are constant: excitatory-to-inhibitory ones are 0.018, inhibitory-to-excitatory 0.002, and inhibitory-to-inhibitory 0.0025 as shown in [6].

2.2. Local projections of inhibitory neurons

In the numerical experiment, we used 10000 excitatory neurons and 2000 inhibitory neurons that are randomly and partially connected. The connection probabilities onto an excitatory and inhibitory neurons are 10 % and 50 %, respectively. Each model neuron was assigned on each coordinate (a, b), a and b are integers, in the square area of $1 \leq x \leq 109$, $1 \leq y \leq 109$ on the x - y plane (Fig.1). The remaining $12000 - 109^2 = 119$ neurons are put along surround of this area. Here, it is possible to define the Euclid distance between neurons using the coordinates. Assuming that an inhibitory neuron and another neuron on which the inhibitory neuron projects are on (x, y) and (x', y'), respectively, we localized the range of projections of inhibitory neurons as anatomically known within the distance, $\sqrt{(x-x')^2 + (y-y')^2} < 87$. The projections from excitatory neurons are free from this constraint. Concretely, inhibitory neurons are divided into 2-to-1 and the localization rule is applied as follows: 1333 inhibitory neurons are randomly connected to all neurons, while the projections from the remaining 667 inhibitory neurons are constrained within the range shown above [7].

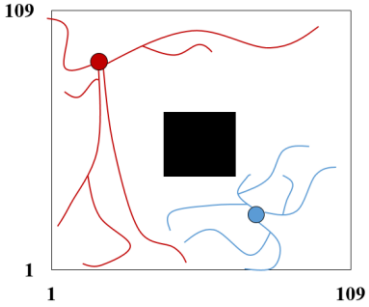

Figure 1: Schematic diagram of two-dimensional neurons

3. Results

3.1. Effects on firing patterns and mean firing rates

During the initial 100 ms, spontaneous activity was driven by the external inputs of Poisson trains to all neurons. After that, we injured 500 neurons in the central region on the plane at $t = 1000$ ms. To make raster plots in injured and uninjured regions easy to discriminate, we have numbered the neurons following the Ulam spiral [8] from the center (Fig.2). In other words, the neurons in the injury region were numbered from 1 to 500. Figure 3 shows examples of raster plots when there is (a) no injury and (b) injured. The vertical axis shows the neuron number and the horizontal axis represents time. As the neuron number is smaller, the neuronal position is closer to the damaged portion. The raster plot with injury showed little effect on the asynchronous spontaneous firing patterns. The mean firing rate and standard deviation of population neurons without injury averaged during $t = 1000$~2000 ms are $1.79 \pm 6.59 \times 10^{-1}$ Hz in excitatory neurons and $14.91 \pm 1.26 \times 10$ Hz in inhibitory ones. With injury, they are $1.73 \pm 6.06 \times 10^{-1}$ Hz and $14.58 \pm 1.18 \times 10$ Hz, respectively. No significant difference was observed in the mean firing rates. The stable mean firing rates also supported asynchronous stability in the case of injury.

65	64	63	62	61	60	59	58	57
66	37	36	35	34	33	32	31	56
67	38	17	16	15	14	13	30	55
68	39	18	5	4	3	12	29	54
69	40	19	6	1	2	11	28	53
70	41	20	7	8	9	10	27	52
71	42	21	22	23	24	25	26	51
72	43	44	45	46	47	48	49	50

Figure 2: Neuron numbering with the Ulam spiral

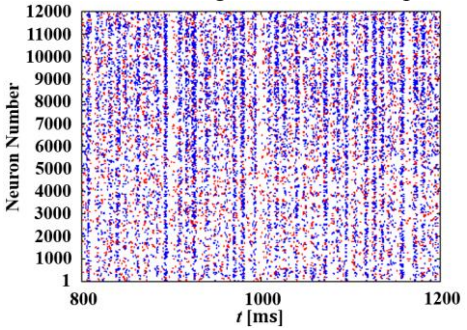

(a) no injury trial

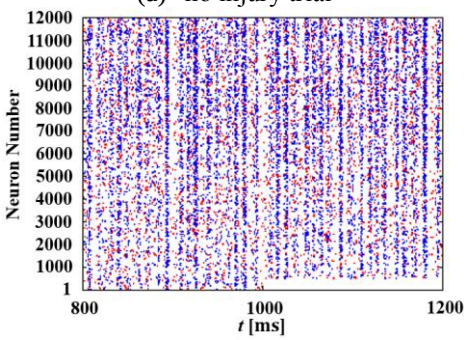

(b) injury trial (injury onset $t = 1000$ ms)

Figure 3: Raster plots with and without injury

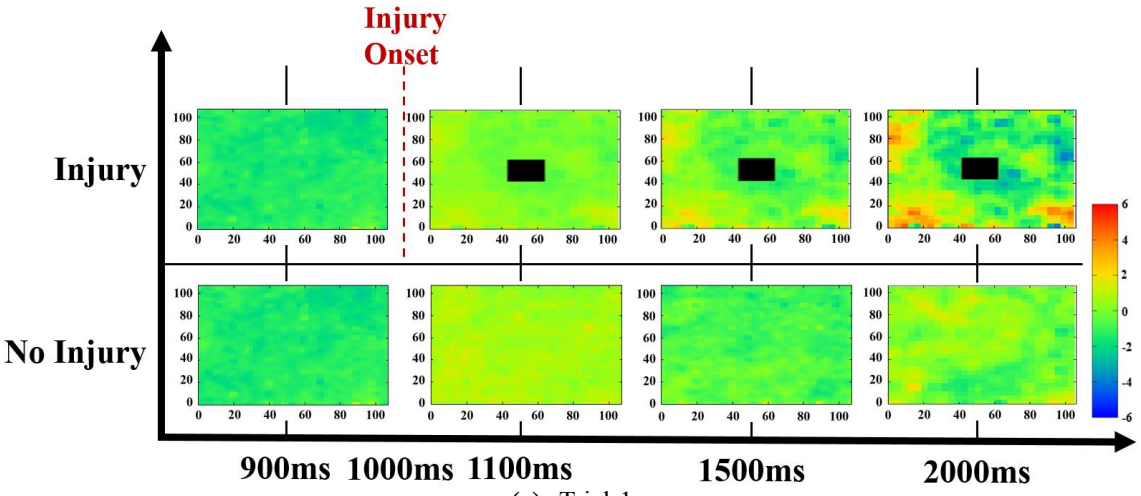

(a) Trial-1

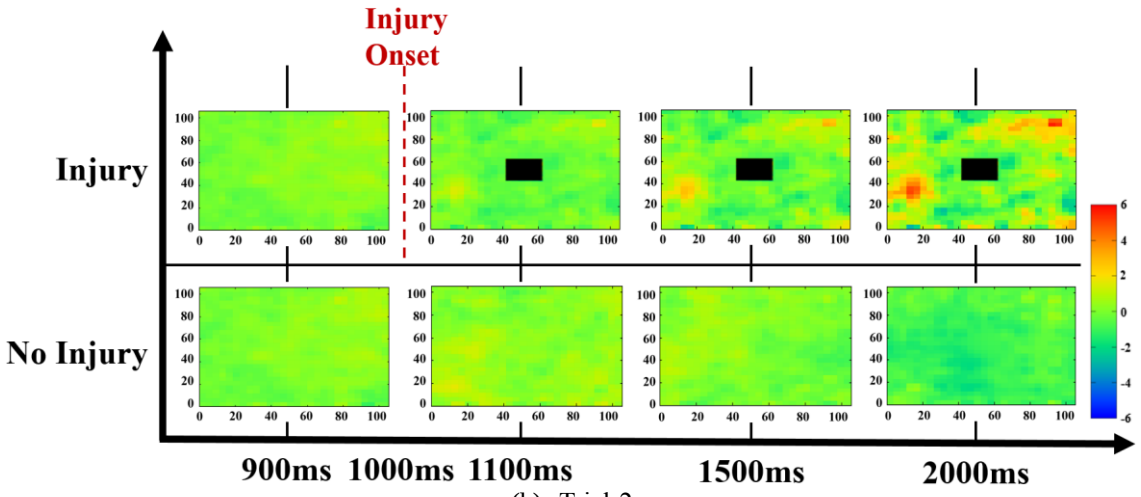

(b) Trial-2

Figure 4: Difference of neuronal activities between injured and uninjured networks

3.2. Increase in neuronal activities around

To visualize the changes of neuronal activities before and after injury in every neuron, the difference (mV) between the mean membrane potential at that time and the baseline potential averaged over pre-injured 500 ms period (t = 500-1000 ms) for each neuron was plotted on the two-dimensional position (Fig.4). Figure 4 (a) is a typical example with and without injury for the same neural network under the condition that they were initially driven by the same Poisson trains for 100 ms. Although the membrane potentials under both conditions hardly differ until t = 1000 ms, the injured network began to show uneven membrane potentials around t = 1500 ms. After all, while the changes in the membrane potentials are relatively smaller and temporary in the uninjured case, some neuronal clusters appeared, whose membrane potentials are increased or decreased in the case of injury. This is because some neurons close to the injury will lose inhibitory inputs from the inhibitory neurons which were in the injured region. Though similar effects from excitatory neurons are possible, the probability that they are injured is low because excitatory connections are not local. The average values of the membrane potential difference of all neurons in t = 2000 ms are -8.02×10^{-2} mV in the case of no injury and 8.28×10^{-2} mV in the case of injury, that shows no significant difference. When a set of driving Poisson trains different from Fig.4 (a) are given to the neural networks with the same synaptic connections as Fig.4 (a), the changes of mean membrane potentials with and without injury are shown in Fig.4 (b). There results indicate that the clusters where neuronal activity is increased or decreased after injury changes their positions in response to the driving input pattern even with the same synaptic connections. This suggests that the areas where their neuronal activities are changed after injury depends on the initial input pattern for driving network as well as its synaptic weight pattern.

3.3. Increased variance of average membrane potentials

As shown above, the average membrane potential in some areas increased or decreased for about 5 mV in the case of injury and this state has continued. This implies that

the distribution of the membrane potentials is extended. Figure 5 shows the normalized frequency distributions of them in the uninjured case (Fig.5 (a)) and injury (Fig.5 (b)) at $t = 2000$ ms. The variance of the distribution in the case of injury is significantly larger in comparison with that without injury ($F(11999,11499) = 3.31$, $P < 0.01$). In addition, while the membrane potentials of the 50 % of all neurons were increased in the case of no injury, 56 % of them were increased in the case of injury. Thus, this may make the populational membrane potential increase after injury as a whole.

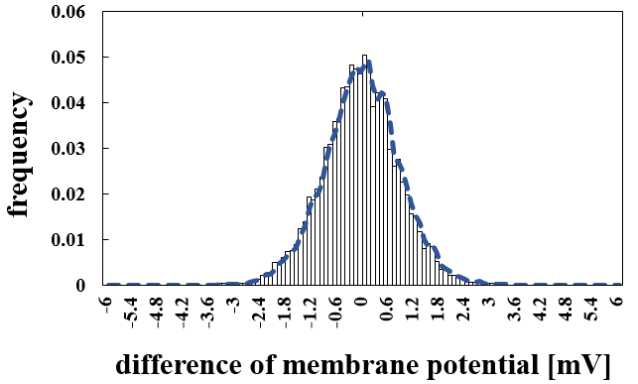

(a) no injury

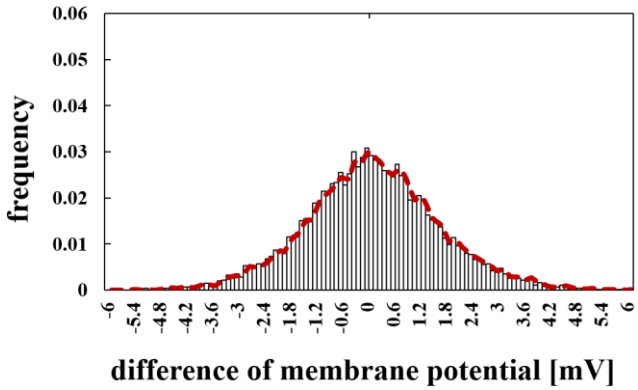

(b) injury

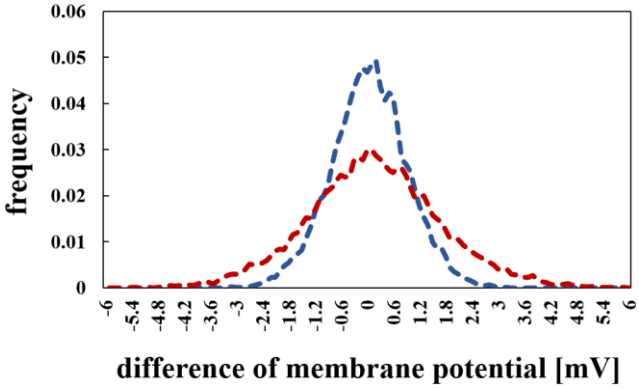

(c) difference of the distributions

Figure 5: Distribution of the difference of membrane potential

4. Conclusion

To simulate remodeling process of the cortex, we injured the neural network model with SSWD and local inhibitory synaptic connections. As a result, increased or decreased average membrane potentials in specific perilesional neuronal populations were observed for seconds only under the injury conditions. The continuous increased activity will be due to more effective loss of the local inhibitory connections to the surrounding neurons than the global excitatory connections. Furthermore, the neurons which receive inhibitory projections directly or indirectly from the activated neurons will remain inhibited. On the other hand, the activated places did not solely depend on the pattern of external inputs or synaptic connections. This suggests that the injured network dynamics has many basins of attraction and that the actual state in the end is determined by the initial driven state in the dynamical system.

References

[1] C. Redecker, H.J. Luhmann, G. Hagemann, J. M. Fritschy and O. W. Witte, "Differential downregulation of GABAA receptor subunits in widespread brain regions in the freeze-lesion model of focal cortical malformations," J. Neurosci., vol.20, no.13, pp.5045-5053, 2000.

[2] D. Ramanathan, J.M. Conner and M.H. Tuszynski, "A form of motor cortical plasticity that correlates with recovery of function after brain injury," Proc Natl Acad Sci U S A, vol.103, no.30, pp.11370-11375, 2006.

[3] S. Lee, M. Ueno and T. Yamashita, "Axonal remodeling for motor recovery after traumatic brain injury requires downregulation of γ-aminobutyric acid signaling," Cell Death & Disease, vol.2, e133, 2011.

[4] H. Einarsdottir, F, Montani, S.R. Schultz, "A mathematical model of receptive field reorganization following stroke," Development and Learning, pp.211-216, 2007.

[5] G.I. Detorakis, N.P. Rougier, "Structure of receptive fields in a computational model of area 3b of primary sensory cortex," Front Comput Neurosci, vol. 8, no.76, 2014.

[6] J.N. Teramae, Y. Tsubo, T. Fukai, "Optimal spike-based communication in excitable networks with strong-sparse and weak-dense links," Scientific Reports, vol.2, no.485, 2012.

[7] Y. Aviel, C. Mehring, M. Abeles, D. Horn, "On embedding synfire chains in a balanced network," Neural Comput, vol.15, pp.1321-1340, 2003.

[8] M.L. Stein, S.M. Ulam, M.B. Wells, "A visual Display of some properties of the distribution of primes," American mathematical monthly, vol.71, no.5, pp.516–520, 1964.